

## IMPACT OF ACETATE IONS ON THE SHAPE OF $\text{Co}_3\text{O}_4$ NANOPARTICLES

E. L. VILJOEN\*, M. J. MOLOTO, P. M. THABEDE

*Chemistry Department, Vaal University of Technology, Private Bag X021, Vanderbijlpark, 1900, South Africa*

Cobalt oxide nanoparticles are materials that have great potential as catalysts for the oxidation of carbon monoxide and hydrocarbons. Cobalt oxide nanoparticles were prepared using a precipitation-oxidation method with  $\text{H}_2\text{O}_2$  at  $85^\circ\text{C}$  and at ambient pressure. The introduction of acetate ions during the precipitation method influenced the shape of the  $\text{Co}_3\text{O}_4$  nanoparticles. TEM analyses indicated that cubic nanoparticles with an average size of 5.1 nm were obtained when the acetate ion was part of the cobalt precursor, cobalt acetate. However, when the acetic acid was added as a capping molecule, spherical nanoparticles with an average size of 4.6 nm were obtained. In the absence of acetate ions, spherical nanoparticles with a size of 6.3 nm were obtained. FTIR spectroscopy and TGA analysis of the nanoparticles indicated that more acetate ions were adsorbed on the surface of the nanoparticles when the acetate ions were introduced through the cobalt precursor, cobalt acetate. It is speculated that the reason for the selective formation of cobalt oxide nanocubes, rather than nanospheres, is due to the higher amount of acetate ions in the precipitate composition and on the surface of the  $\text{Co}_3\text{O}_4$  nanoparticles.

(Received March 23, 2017; Accepted June 7, 2017)

*Keywords:* Nanoparticles, Nanodots,  $\text{Co}_3\text{O}_4$ , Morphology, Acetate ions

### 1. Introduction

Cobalt oxide nanoparticles can be used for various applications, for example as catalysts, [1-6] in electrochemical detection [7] and in batteries [8]. Their size and shape affects the properties of the cobalt nanoparticles. Catalytic activity normally increases with a decrease in size due to the higher surface area which results from the smaller nanoparticles. The catalytic activity for ozonation of phenol was much higher for  $\text{Co}_3\text{O}_4$  nanoparticles than for bulk  $\text{Co}_3\text{O}_4$  [1] and the activity further increased with a decrease in the cobalt oxide spherical nanoparticle size from 70 to 3.5 nm [2]. The catalytic activity for the photo-catalytic oxidation of black dye increased when the  $\text{Co}_3\text{O}_4$  nanorod size decreased from 35 to 15 nm [3]. The shape of nanoparticles also change the activity of  $\text{Co}_3\text{O}_4$  since different Miller indices are exposed on differently shaped nanoparticles. Nanocubes made of  $\text{Co}_3\text{O}_4$  had better sensitivity and lower detection limits than  $\text{Co}_3\text{O}_4$  nanospheres for the electrochemical detection of hydrogen peroxide [7].  $\text{Co}_3\text{O}_4$  nanoparticles exposing {111} Miller indices were more effective in reducing the discharge charge over-potential in  $\text{Li-O}_2$  batteries than nanoparticles exposing {100}, {110} and {112} surface planes [8]. The catalytic activity for methane combustion of nanosheets with {112} surfaces were higher than nanorods with {110} surface planes and nanocubes with {100} surfaces [4]. The catalytic activity for CO oxidation using nanorods with surfaces {110} was higher than for truncated octahedra with {111} and {100} surfaces [5].  $\text{Co}_3\text{O}_4$  nanorods with surfaces {110} were more active than nanoparticles with {100} and {111} surfaces for the catalytic reduction of nitrogen oxides by ammonia [6]. When the cobalt oxide nanoparticles are to be used as catalysts, complex capping molecules strongly adsorbed on the surface is undesirable since the capping molecule can lead to a decrease in the activity of the catalyst. It is thus important to investigate and develop preparative

---

\* Corresponding author: elverav@vut.ac.za

methods that can produce nanoparticles of different sizes and shapes without the use of complex capping molecules.

Cobalt oxide ( $\text{Co}_3\text{O}_4$ ) nanoparticles with cubic shapes between 3.5-5.7 nm were formed when TWEEN-85, polyoxyethylene (20) sorbitan trioleate, was used as capping molecule [9]. The results of Xu and Zeng [9] indicate that the TWEEN-85, which is an ester, hydrolysed forming a carboxylate ion (oleate ion) which adsorbed on the cobalt oxide surface. Cubic shaped cobalt oxide of about 18 nm were also obtained when cobalt acetate were used instead of cobalt nitrate and cobalt sulphate [10]. It may be deduced from the results of Xu and Zeng [9] and Yang et al. [10], that cubic cobalt oxide nanoparticles can thus be produced in the presence of carboxylate ions using a precipitation-oxidation method. The carboxylate ion can be introduced as a capping molecule or as part of the cobalt precursor. This study thus investigated the influence of the acetate ion on the size and shape of the cobalt oxide nanoparticles in the form of acetic acid (capping molecule) and cobalt acetate precursor.

## 2. Experimental Section

### 2.1 Materials

Cobalt nitrate hexahydrate,  $\text{Co}(\text{NO}_3)_2 \cdot 6\text{H}_2\text{O}$ , 97% was purchased from BDH Lab Suppliers. Hydrogen peroxide ( $\text{H}_2\text{O}_2$  in water, 30%) and sodium hydroxide (NaOH, 99.5%) were obtained from Labo-Chem. Hydrochloric acid (HCl, 32%), 1-butanol (99.8%) and methanol (99.5%) were bought from Laboratory Consumables and Chemicals. Cobalt acetate tetrahydrate ( $\text{Co}(\text{CH}_3\text{COO})_2 \cdot 4\text{H}_2\text{O}$ , 99.999%) was purchased from Sigma. Acetic acid ( $\text{CH}_3\text{COOH}$ , 98%) was procured from Promark Chemicals. All chemicals were used without further purification.

The preparation method of the  $\text{Co}_3\text{O}_4$  nanoparticles was based on a combination of the methods of Xu and Zeng [9] and Yang et al. [10]. Butanol instead of polyethylene glycol (PEG) was added to the reaction mixture [10]. A temperature of 85 °C, similar to Xu and Zeng [9] was used. Yang et al. [10] used a higher temperature of 160 °C and a higher pressure since an autoclave was used. Xu and Zeng [9] used air as oxidant whereas in this study,  $\text{H}_2\text{O}_2$  was used like Yang et al. [10] did. In this study 20% excess of  $\text{H}_2\text{O}_2$  was added than the theoretically required amount for the formation of  $\text{Co}_3\text{O}_4$  (based on redox half reactions) since  $\text{H}_2\text{O}_2$  decomposes when mixed with the cobalt salt. The unreacted cobalt hydroxide was dissolved using diluted hydrochloric acid as described in the method of Xu and Zeng [9].

### 2.2 Preparation of Nanoparticles

Cobalt nitrate (5.8193 g) dissolved in 10 ml of water and hydrogen peroxide solution (0.9102 g) diluted with 10 ml of water, were mixed together. Sodium hydroxide (1.2689 g) was dissolved in 100 ml of water. Butanol (20 ml) and the mixture of cobalt nitrate/hydrogen peroxide were added to the sodium hydroxide solution. The solution contained in a three neck round bottom flask was placed in an unheated oil bath and stirred with a magnetic stirrer. The oil was then heated to obtain a reaction mixture temperature of 85 °C and the mixture was kept at 85 °C for 16 hours. The solution was allowed to cool to room temperature and centrifuged at 5000 rpm for 5 minutes. The solid product was washed three times with 50 ml 2 M HCl to dissolve the unreacted cobalt hydroxide compounds. The product was washed twice with 50 ml of water and finally the solid product (sample A) was washed once with 50 ml of methanol. The nanoparticles produced were left at room temperature do dry.

The same procedure was used to prepare  $\text{Co}_3\text{O}_4$  nanoparticles from cobalt acetate instead of cobalt nitrate (sample B). A mass of 4.9816 g of the  $\text{Co}(\text{CH}_3\text{COOH})_2 \cdot 4\text{H}_2\text{O}$  was used to obtain the same mole amount of  $\text{Co}^{2+}$ . The same procedure was also used to prepare  $\text{Co}_3\text{O}_4$  nanoparticles from cobalt nitrate mixed with acetic acid instead of cobalt nitrate (sample C). Acetic acid (2.4562 g) was added as capping molecule to the cobalt nitrate solution. More NaOH (2.9338 g) was used to neutralise the acetic acid in order to precipitate at a similar pH.

### 2.3 Nanoparticle characterisation

UV-Vis spectroscopy analyses were performed with a double beam spectrometer - Perkin Elmer Lambda 25 UV/Vis, with a tungsten and deuterium lamp, which collects spectra from 180-1100 nm wavelength using a bandwidth of 1 nm with a fixed slit. A baseline setting was done by using pure water as a reference sample. A very small amount of the solid sample/crystals was dispersed in water. A Gaussian peak was fitted to the adsorption peak with the program Fityk to obtain the peak maximum position.

XRD analyses were done using the Shimadzu-XRD 700, X-Ray Diffractometer with Cu K $\alpha$  radiation ( $\lambda = 1.154056 \text{ \AA}$ ). A scan speed of  $1^\circ/\text{minute}$ , current 30 mA and voltage of 40 kV were used. The FWHM (Full-Width Half-Maximum) was determined by fitting a Gaussian peak using the Fityk program. The FWHM was used to calculate the average crystallite size using the Scherrer equation  $D = K\lambda/\beta\cos\theta$ . A value of 0.9 was used for the Scherrer constant K,  $1.154056 \text{ \AA}$  for  $\lambda$ ,  $\beta$  is the line width FWHM as  $2\theta$ ,  $\theta$  is the Bragg angle, and D is the crystallite size. The strongest diffraction peak, (311), at  $\sim 36^\circ 2\theta$  in the XRD diffraction pattern were used to calculate the average crystallite size. Peak broadening due to the instrument and strain have not been taken into account, thus the size calculated from XRD will give a smaller size than the actual size.

FTIR (Fourier transform infrared) spectra was measured using a Perkin Elmer Spectrum 400 FT-IR/FT-NIR Spectrometer, universal ATR with diamond detector and a wavelength scan range from  $650 \text{ cm}^{-1}$  to  $4000 \text{ cm}^{-1}$ . A Perkin Elmer, STA 6000 simultaneous Thermal Analyser TGA was used. The temperature was increased from  $30^\circ\text{C}$  to  $900^\circ\text{C}$  using a ramp rate of  $10^\circ/\text{minute}$  with a nitrogen flow rate of  $20 \text{ ml/minute}$ . A sample mass between 7 and 13 mg were used.

The size and shape of the dried supported nanoparticles were determined using a Transmission Electron Microscope, LEO TEM 912, with an acceleration voltage of 120 kV and a tungsten wire filament. The nanoparticles dispersed in the methanol were pipetted onto carbon-coated, copper grids and allowed to dry. The nanoparticles' sizes were measured using the software program ImageJ.

### 3. Results and discussion

The XRD diffraction patterns (see Figure 1) show the cobalt oxide phase of the nanoparticles is  $\text{Co}_3\text{O}_4$  (PDF card number 00-042-1467) in all the samples. TEM and XRD indicated that the sizes obtained from the different preparation methods were similar (see Table 1), with the nanoparticles made from cobalt nitrate being slightly larger and nanoparticles made from the combination of cobalt nitrate and acetate being slightly smaller. The sizes obtained by XRD were slightly smaller than those obtained by TEM, and it may be due to peak broadening from to the instrument and strain not taken into account. The nanoparticles made from cobalt acetate were cubic in shape, in contrast to the spherical shapes of the nanoparticles prepared with the other two methods as determined by TEM (see Figure 2).

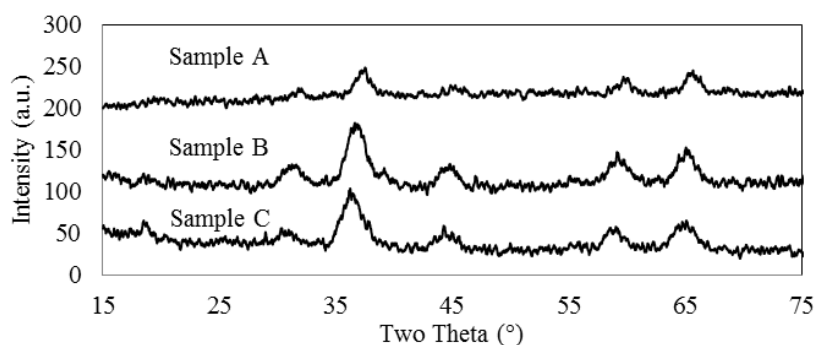


Fig. 1. X-ray Diffraction pattern of the  $\text{Co}_3\text{O}_4$  nanoparticles prepared at  $85^\circ\text{C}$  for 16 hours from (A)  $\text{Co}(\text{NO}_3)_2 \cdot 6\text{H}_2\text{O}$ , (B)  $\text{Co}(\text{CH}_3\text{COO})_2 \cdot 4\text{H}_2\text{O}$  and from (C)  $\text{Co}(\text{NO}_3)_2 \cdot 6\text{H}_2\text{O}$  with  $\text{CH}_3\text{COOH}$

Table 1: Nanoparticle size determination with XRD and TEM

	Nanoparticles prepared from cobalt nitrate (Sample A)	Nanoparticles prepared from cobalt acetate (Sample B)	Nanoparticles prepared from cobalt nitrate and acetic acid (Sample C)
XRD size (nm)	5.8	4.5	4.3
TEM size (nm)	6.3	5.1	4.6
TEM standard deviation (nm)	1.2	0.7	1.0

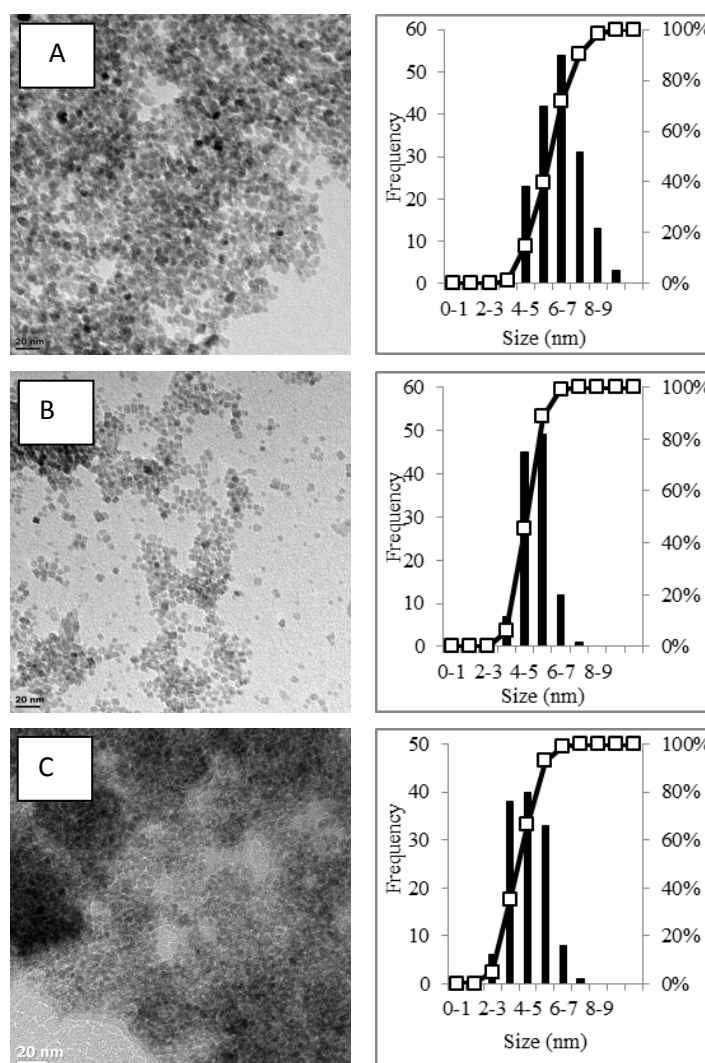


Fig. 2. TEM analyses of Sample A,  $\text{Co}_3\text{O}_4$  nanoparticles from  $\text{Co}(\text{NO}_3)_2 \cdot 6\text{H}_2\text{O}$ , Sample B,  $\text{Co}_3\text{O}_4$  nanoparticles prepared from  $\text{Co}(\text{CH}_3\text{COO})_2 \cdot 4\text{H}_2\text{O}$  Sample C,  $\text{Co}_3\text{O}_4$  nanoparticles prepared from  $\text{Co}(\text{NO}_3)_2 \cdot 6\text{H}_2\text{O}$  and  $\text{CH}_3\text{COOH}$ .

The optical properties of the nanoparticles were characterised using UV-Vis spectroscopy (Figure 3). The peak around 450 nm can be ascribed to the ligand to metal charge transfer transition;  $\text{Co}^{3+} \leftarrow \text{O}^{2-}$  and the peak around 725 nm can be ascribed as due to the ligand to metal charge transfer transition;  $\text{Co}^{2+} \leftarrow \text{O}^{2-}$  [11]. The third peak around 975 nm for the  $\text{Co}_3\text{O}_4$  nanoparticles prepared from cobalt acetate (Sample B) can be interpreted as a charge transfer transition  $\text{Co}^{2+} \leftarrow \text{Co}^{3+}$  [11].

The size and shape of a nanoparticle are known to influence the band gap [9]. A decrease in the size of the nanoparticle results in an increase in the band gap [9]. TEM analyses showed that a range of sizes for the nanoparticles were present in the samples (Figure 2) and therefore a range of band gaps will be obtained which will lead to a broad absorption peak in the UV-Vis spectra as observed in Figure 3. The peak maximum of the absorption peak may be interpreted as the band gap of the most abundant size of nanoparticles. The band gap for the most abundant nanoparticle size is 2.61 eV and 1.63 eV for the  $\text{Co}_3\text{O}_4$  nanoparticles prepared from cobalt nitrate (Sample A); 2.97 eV, 1.72 eV and 1.27 eV for the  $\text{Co}_3\text{O}_4$  nanoparticles prepared from cobalt acetate (Sample B) and 3.05 and 1.77 eV for the  $\text{Co}_3\text{O}_4$  nanoparticles prepared from cobalt nitrate and acetic acid (Sample C). Bulk  $\text{Co}_3\text{O}_4$  has band gaps at 2.19 eV and 1.48 eV [12]. The absorption peaks of the nanoparticles have been blue shifted in comparison to the absorption peaks of bulk  $\text{Co}_3\text{O}_4$  showing that the smaller sizes of cobalt oxide nanoparticles resulted in an increased band gap.

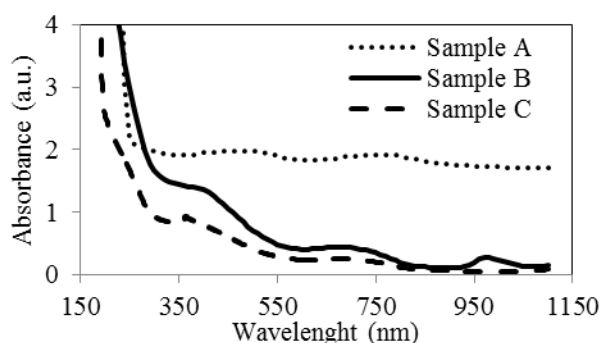


Fig. 3. UV-vis spectra of  $\text{Co}_3\text{O}_4$  nanoparticles prepared at  $85^\circ\text{C}$  for 16 hours. Sample A prepared from  $\text{Co}(\text{NO}_3)_2 \cdot 6\text{H}_2\text{O}$ , Sample B prepared from  $\text{Co}(\text{CH}_3\text{COO})_2 \cdot 4\text{H}_2\text{O}$  and Sample C prepared from  $\text{Co}(\text{NO}_3)_2 \cdot 6\text{H}_2\text{O}$  and  $\text{CH}_3\text{COOH}$ .

TGA was conducted to determine how much anions were adsorbed on the cobalt oxide surface. The first peak around  $100^\circ\text{C}$  and the last peak around  $800^\circ\text{C}$  may be ascribed to water desorption, and  $\text{Co}_3\text{O}_4$  decomposing to  $\text{CoO}$ , respectively. Since the decomposition temperature of cobalt acetate ( $252^\circ\text{C}$ ) is higher than that of cobalt nitrate ( $200^\circ\text{C}$ ) as measured by TGA [13], the peaks around  $300^\circ\text{C}$  and  $150^\circ\text{C}$  were ascribed to the desorption of the acetate ion and the nitrate ions, respectively, from the cobalt oxide nanoparticle surfaces (see Figure 4). The higher desorption temperature of the acetate ion in comparison to the nitrate ion may indicate that the adsorption of the acetate ion on the cobalt oxide surface is stronger than the adsorption of the cobalt nitrate ion on the cobalt oxide surface.

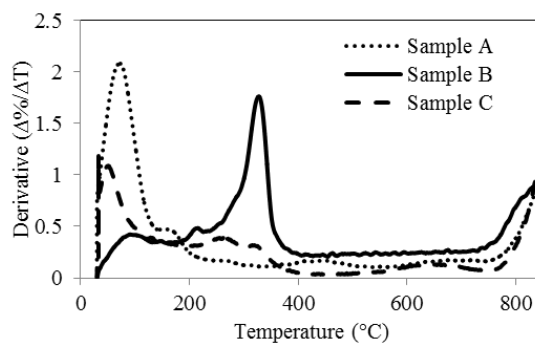


Fig. 4. TGA analyses of the  $\text{Co}_3\text{O}_4$  nanoparticles prepared at  $85^\circ\text{C}$  for 16 hours. Sample A prepared from  $\text{Co}(\text{NO}_3)_2 \cdot 6\text{H}_2\text{O}$ , Sample B prepared from  $\text{Co}(\text{CH}_3\text{COO})_2 \cdot 4\text{H}_2\text{O}$  and Sample C prepared from  $\text{Co}(\text{NO}_3)_2 \cdot 6\text{H}_2\text{O}$  and  $\text{CH}_3\text{COOH}$ .

The small peak at about  $1760\text{ cm}^{-1}$  present in the FTIR spectra (Figure 5), may be assigned to C=O stretch. The O-H bending modes of adsorbed water give broad peaks around  $1630\text{ cm}^{-1}$  [10]. The peaks at about  $1555\text{ cm}^{-1}$  can be ascribed to  $\text{COO}^-$  asymmetrical stretching [14]. The broad peak at  $1421\text{ cm}^{-1}$  seems to be a combination of more than one peak and may be ascribed to  $\text{COO}^-$  symmetrical stretching modes and the C-H bending mode [14]. The peak at  $1368\text{ cm}^{-1}$  may also be ascribed to C-H bending mode [14]. The later peak is however close to the vibrational peak of  $\text{NO}_3^-$  which is at  $1351\text{ cm}^{-1}$  [10]. The  $\text{COO}^-$  asymmetrical stretching mode at about  $1555\text{ cm}^{-1}$  is thus the most useful peak to judge the relative amount of acetate ions adsorbed on the cobalt oxide nanoparticles. This peak indicates that there is more acetate ions adsorbed on the surface of the cobalt nanoparticles made from cobalt acetate (sample B) in comparison to the nanoparticles made from the mixture of cobalt nitrate and acetic acid mixture (sample C). Both nitrate and acetate anions are present on the surface of the cobalt nanoparticles (sample C) made from cobalt nitrate and acetic acid.

Both the TGA and FTIR spectroscopy results indicate that there are more adsorbed acetate ions on the surface for the cobalt oxide nanoparticles made from cobalt acetate (sample B) in comparison to the nanoparticles made from the mixture of cobalt nitrate and acetic acid (sample C), even though the acetate : cobalt mole ratio was 2:1 in both cases. The stronger adsorbed acetate ions and the higher amount of acetate ions on the cobalt oxide nanoparticles made from cobalt acetate may be the cause of selectively obtaining cubic shapes instead of spherical shapes. Capping molecules (acetate ions in this case) adsorbed on surfaces can change the nanoparticles' shape as reported by Xiao et al. [15]. Shape control can take place either kinetically or thermodynamically [15].

The precipitate composition is expected to be different since the amount of sodium hydroxide is not enough to form  $\text{Co}(\text{OH})_2$  or  $\text{Co}(\text{OH})_3$  which means the nitrate and acetate ions would also form part of the precipitate composition leading to different precipitation compositions for the three methods used. Yang et al. [10] proposed that the different precipitate compositions may be the cause of different shapes of  $\text{Co}_3\text{O}_4$  nanoparticles formed.

The adsorbed acetate ions (samples B and C) when cobalt acetate and a mixture of cobalt nitrate and acetic acid were used, caused a decrease in the rate of reaction resulting in the slightly smaller average nanoparticle sizes. The ionic strength was also higher in the case where a mixture of cobalt nitrate and acetic acid were used (sample C), which resulted in the decrease in the size of nanoparticles [16].

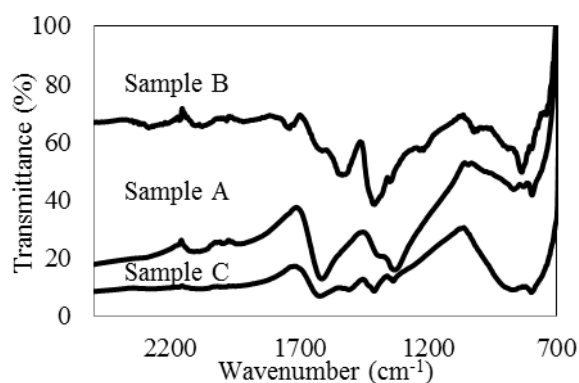


Fig. 5. FTIR spectra of  $\text{Co}_3\text{O}_4$  nanoparticles prepared at  $85^\circ\text{C}$  for 16 hours. Sample A prepared from  $\text{Co}(\text{NO}_3)_2 \cdot 6\text{H}_2\text{O}$ , Sample B prepared from  $\text{Co}(\text{CH}_3\text{COO})_2 \cdot 4\text{H}_2\text{O}$  and Sample C prepared from  $\text{Co}(\text{NO}_3)_2 \cdot 6\text{H}_2\text{O}$  and  $\text{CH}_3\text{COOH}$ .

#### 4. Conclusions

The manner in which the acetate ion is introduced during the preparation method has a direct influence on the shape of the nanoparticles obtained. The addition of the acetate ion as part of the cobalt precursor resulted in cubic shaped  $\text{Co}_3\text{O}_4$  nanoparticles with a size of 5.1 nm. In the

absence of the acetate ion, and when the acetate ion was introduced by the addition of acetic acid, spherical shaped nanoparticles were formed in both cases. The precipitate compositions, higher strength of adsorption and the higher amount of acetate ions adsorbed on the  $\text{Co}_3\text{O}_4$  nanoparticles (when the nanoparticles were made from cobalt acetate) may have resulted in the preferential formation of cubic shaped particles. The advantage of this method is that both cubic and spherical nanoparticles of cobalt oxide (smaller than 10 nm in size) can be selectively prepared in the absence of complex capping molecules, using mild reaction conditions.

### Acknowledgements

National Research Foundation (NRF) study bursary for Mapule Thabede. This work is based on the research supported in part by the National Research Foundation of South Africa for the grant, Unique Grant No. 99330.

### References

- [1] Y. Dong, G. Wang, P. Jiang, A. Zhang, L. Yue, X. Zhang, *Bull. Korean Chem. Soc.* **31**(10), 1 (2010).
- [2] Y. Dong, K. He, L. Yin, A. Zhang, *Nanotechnology* **18**, 435602 (2007).
- [3] H. Li, G.T. Fei, M. Fanga, P. Cuia, X. Guoa, P. Yana L.D. Zhang, *Appl. Surf. Sci.* **257**, 6527 (2011).
- [4] L. Hu, Q. Peng, Y. Li, *J. Am. Chem. Soc.* **130**, 16136 (2008).
- [5] X. Xie, W. Shen, *Nanoscale* **1**, 50 (2009).
- [6] B. Meng, Z. Zhao, X. Wang, J. Liang, J. Qiu, *Appl Catal B.* **129**, 491 (2013).
- [7] S. Xia, M. Yu, J. Hu, J. Feng, J. Chen, M. Shi, X. Weng, *Electrochem Commun.* **40**, 67 (2014).
- [8] D. Su, S. Dou, G. Wang, *Nature Scientific Reports, AP Energy* **4**, 5767 (2014).
- [9] R. Xu, H.C. Zeng, *Langmuir* **20**, 9780 (2004).
- [10] Y.P. Yang, R.S. Liu, K.L. Huang, L.P. Wang, S.Q. Liu, W.W. Zeng, *Trans. Nonferrous Met. Soc. China* **17**, 1334 (2007).
- [11] S. Thota, A. Kumar, J. Kumar, *Mater. Sci. Eng. B.* **164**, 30 (2009).
- [12] M. Salavati-Niasari, N. Mir, F. Davar, *J. Phys. Chem. Solids.* **70**, 847 (2009).
- [13] A.Y. Khodakov, J.S. Girardon, A. Griboval-Constant, A.S. Lermontov, P.A. Chernavskii, *Stud Surf Sci Catal.* **147**, 295 (2004).
- [14] Z. Nickolov, G. Georgiev, D. Stoilova, I. Ivanov, *J Mol Struct.* **354**, 119 (1995).
- [15] J. Xiao, L. Qi, *Nanoscale.* **3**, 1383 (2011).
- [16] M. Mohapatra, S. Anand, *IJEST* **2**( 8), 127 (2010).